Studies of N-Terminal Templates for α-Helix Formation. Synthesis and Conformational Analysis of (2S,5S,8S,11S)-1-Acetyl-1,4-diaza-3-keto-5-carboxy-10-thiatricyclo[2.8.1.0^{4,8}]-tridecane (Ac-Hel$_1$-OH)

D. S. Kemp,* Timothy P. Curran, William M. Davis, James G. Boyd, and Christopher Muendel

Room 18-582, Department of Chemistry, Massachusetts Institute of Technology, Cambridge, Massachusetts 02139

Received January 23, 1991 (Revised Manuscript Received July 1, 1991)

A convergent synthesis of the title compound, a conformationally restricted analogue of acetyl-L-prolyl-L-proline, from 1-acetyl-2(*S*)-carboxy-4(*S*)-mercaptopyrrolidine and *trans*-1-(*tert*-butoxycarbonyl)-2(*S*)-(methoxycarbonyl)-5(*S*)-[(tosyloxy)methyl]pyrrolidine (Ac-Hel$_1$-OH) is reported, along with a synthesis of (2*S*,8*S*,11*S*)-1-acetyl-1,4-diaza-3-keto-10-thiatricyclo[2.8.0^{4,8}]tridecane. In the crystal and in $CDCl_3$ solution the conformation of Ac-Hel$_1$-OH is shown to approximate a staggered orientation at the 8,9-CC bond and an s-cis orientation at the acetyl amide bond. In DMF, DMSO, MeCN, and D_2O significant amounts of the s-trans conformer are also present.

Soluble oligopeptides of proper amino acid composition under appropriate aqueous conditions readily forego the random coil state and form structurally well-defined α-helices.[1] By contrast, helical conformation of short- or medium-sized peptides are not normally stable in aqueous solutions, as first noted by Goodman and Schmidt[2] and later confirmed by many workers.[3] The stabilizing features of peptide helices and the rules governing their formation were first deduced from the properties of helical oligopeptides in solution, notably by Scheraga and coworkers.[4] Statistical analyses[5,6] of the frequencies of occurrence of the amino acids in the helical sequences found in globular proteins as analyzed by X-ray crystallography yield parameters that are in reasonably satisfactory agreement with those obtained from oligopeptide studies.

Recent observations by Baldwin and other workers on analogues of the S- and C-peptides formed from ribonuclease A,[7] which show unusually strong temperature-dependent stability in water, and by DeGrado,[8] who has noted remarkable resistance to urea denaturation for rationally designed folded helix bundles, have called into question the relevance of stabilization parameters derived from macromolecular studies when applied to peptide-derived helices of the lengths normally seen in proteins. A tractable low molecular weight model for helix formation that permits conformational scrutiny by the incisive spectroscopic tools of the organic chemist could provide unique insight into the formation of secondary structure during the protein folding process.

In this paper, we report the synthesis and conformational analysis of a constrained analogue of prolylproline that has the potential for nucleation of helices in polypeptides linked to it at their N-termini. In subsequent papers we report and quantitate helix formation for such template-peptide chimeric conjugates in a variety of organic solvents as well as in water.

Design Considerations

The Zimm-Bragg analysis and related models for the helix-coil transition for oligopeptides in water postulate that helix growth results from propagation of a structural interaction between neighboring amino acid residues along the peptide backbone.[9] In these models, helix initiation

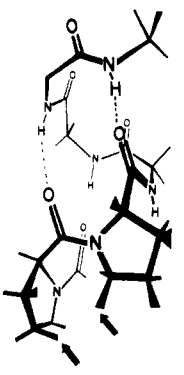

1

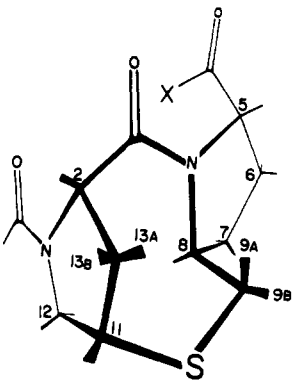

2a (X = OCH_3)
b (X = OH)
c (X = $NHCH_3$)

is seen as an unlikely step, reflecting the difficulty of forming an entropically unfavorable helical orientation at six single backbone bonds of three consecutive amino acid residues. Experimental estimates of this orientation factor, expressed as an equilibrium constant σ, typically lie in the range of 10^{-3} to 10^{-4}.[1,4]

If these models are correct, then properly chosen rigid peptide analogues, characterized by torsional φ and ψ angles that are fixed at helical values, should exhibit σ values close to 1 and initiate helices when attached to short polypeptides of normal structure. We term such a rigid peptide analogue that shows nucleating power a *helical template*. Although one can envisage subclasses of templates that can initiate helices at a peptide N-terminus, at a C-terminus, or from the center of a peptide, the structural constraints required to realize these three classes

(1) Doty, P.; Wada, A.; Yang, J. T.; Blout, E. *J. Polymer Sci.* **1957**, *23*, 851. Gratzer, W. B.; Doty, P. *J. Am. Chem. Soc.* **1963**, *85*, 1193.
(2) Goodman, M.; Schmitt, E. E.; Yphantis, D. A. *J. Am. Chem. Soc.* **1962**, *84*, 1962.
(3) Naider, F.; Goodman, M. Conformational Analysis of Oligopeptides by Spectroscopic Techniques. In *Biorganic Chem.* Van Tamelen, E. E., Ed.; Academic Press: New York, 1977; Vol. III, p 177. Yaron, A.; Katchalski, E.; Berger, A.; Fasman, G. D.; Sober, H. A. *Biopolymers* **1971**, *10*, 1107. Epand, R.; Scheraga, H. A. *Biochemistry* **1968**, *7*, 284. Panijpan, B.; Gratzer, W. *Eur. J. Biochem.* **1974**, *45*, 547. Boesch, S.; Bundi, A.; Opplinger, M.; Wuethrich, K. *Eur. J. Biochem.* **1978**, *91*, 209.
(4) Scheraga, H. A. *Pure Appl. Chem.* **1978**, *50*, 315. Go, M.; Scheraga, H. A. *Biopolymers* **1984**, *23*, 1961.
(5) Chou, P.; Fasman, G. D. *Adv. Enzymol.* **1978**, *47*, 45.
(6) Levitt, M. *Biochem.* **1978**, *17*, 4277.
(7) Bierzynski, A.; Kim, P. S.; Baldwin, R. L. *Proc. Nat. Acad. Sci. U.S.A.* **1982**, *79*, 2470. Marqusee, S.; Baldwin, R. L. *Proc. Nat. Acad. Sci. U.S.A.* **1989**, *86*, 5286. Nelson, J. W.; Kallenbach, N. R. *Proteins* **1988**, *1*, 211-217. Merutka, G.; Stellwagen, E. *Biochem.* **1989**, *28*, 353-357.
(8) Ho, S. P.; DeGrado, W. F. *J. Am. Chem. Soc.* **1987**, *109*, 6751.
(9) Zimm, B. H.; Bragg, J. *J. Chem. Phys.* **1959**, *31*, 526. Lifson, S.; Roig, A. *J. Chem. Phys.* **1961**, *34*, 1963.

0022-3263/91/1956-6672$02.50/0

are very different. Nucleation within the center of a peptide is envisaged most easily by side-chain constraints and has been reported recently by two groups.[10] Nucleation at the C-terminus of a peptide cannot be achieved easily by small rings joined to the atoms of the peptide backbone since oxygen, the obvious linkage site, is bivalent. Either side-chain constraints or cyclic heteroatom analogues of secondary amides such as amidines must be used to realize templates at this site. By contrast, nucleation at the N-terminus can involve conformational constraints that can establish a helical geometry by means of ring-locked tertiary amide functions. As noted by a number of workers, nature probably uses proline residues for this purpose.[5,6,11]

A classical right-handed α-helix has ϕ and ψ values of −57° and −47°,[12] respectively. The pyrrolidine ring of a proline residue constrains its ϕ value to approximately −60°, and as noted in 1, our first exercise in the design of helical templates used the strategy of adding further structural constraints to the atomic linkages of Ac-L-Pro-L-Pro. Although bridges between the 5-site of proline-2 and any among the 3-, 4-, and 5-sites of proline-1 can generate potential helical templates, a two-atom bridge between site 3 of proline-1 and site 5 of proline-2 appears to offer maximum rigidity and compliance with the desired dihedral angle of −47° at the Cα–CO bond of proline-1. Longer bonds than those formed by second-row elements were desirable for the two-atom bridge. A sulfur atom was a natural choice in the form of a thiamethylene group, which also permitted use of the readily available *cis*-4-mercapto-L-proline as a synthetic intermediate. The proposed helical template is shown without peptide linkage in 2 and with a linked tripeptide in an α-helical conformation in 3.

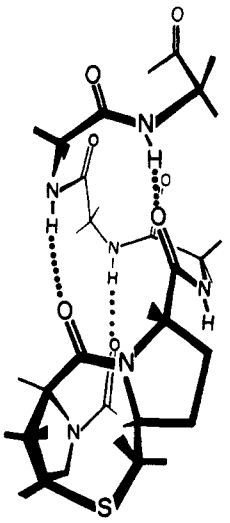

3

The template portion of structure 3 has a number of degrees of conformational freedom. First, the Cα–CO bond that links peptide and template is expected to be subject only to the constraint of a normal proline ψ bond. Second, the acetamido CO–N bond can assume s-cis and s-trans orientations. Third, the eight-membered lactam can flex between a pair of orientations, moving the pyrrolidine ring of proline-1 and its linked acetamido group through a 5–10° arc. Owing to subtle changes of torsional and van der Waals strain within the lactam it is difficult to estimate the stable conformation of this function without a detailed energetic analysis. The results of a conformational analysis of 2 using molecular mechanics, as well as pertinent ^{1}H NMR and X-ray structural data are given in a later section of this paper.

The template 2 provides three amide carbonyls that can assume helical pitch and spacing. Four amide carbonyls are in fact involved in hydrogen-bonding interactions at the N-terminus of an α-helix. For the α-helix 3 to form, the NH of the first template-linked amino acid residue must forego intramolecular hydrogen bonding. Alternatively, the structure may adopt a hybrid 3_{10}-α helical conformation that has been observed in the crystalline state in protein structures[13] and model peptides.[14]

The template 2 has been designed around a local, tricyclic constraint, which is probably one of the simplest ways one might nucleate a helix starting from the N-terminus of a peptide. Other approaches to helical design at the N-terminus include replacement of backbone (i, i + 4) hydrogen bonds with covalent linkages as recently reported by Arrhenius, Lerner, and Satterthwait,[15] and construction of proline-containing macrocycles that enforce helical character.[16] Data from peptide-template conjugates of diverse structural classes will be required to establish those properties that are unique to the helix itself and not artifacts of the structure that initiates it.

Can Ac-Pro-Pro itself serve as a helical template? In properly chosen solvents the answer may be yes[17], but data that will be reported elsewhere establishes that this function shows no detectable tendency to induce helix formation in linked polypeptides in aqueous solution. Evidently, fixing of two single bonds of the peptide backbone in a helical orientation is insufficient to enforce helicity in an aqueous environment.

Synthesis

We have previously reported in outline a synthesis of 2 culminating in thioether formation between the two functionalized pyrrolidines (*S*,*S*)-4 and (*S*,*S*)-5, followed by carboxyl activation, urethane cleavage, and closure of the lactam ring.[18] Although the synthesis of (*S*,*S*)-4 in

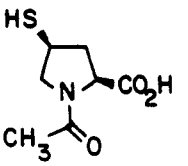

(S,S)-4

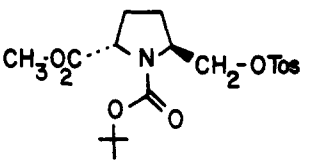

(S,S)-5

six steps from L-hydroxyproline has been previously described by Eswarakrishnan anf Field,[19] we modified this route as shown in Scheme I, replacing diazomethane with

(10) Madison, V. S.; Fry, D. C.; Greeley, D. N.; Toome, V.; Wegrzynski, B. B.; Heimer, E. P.; Felix, A. M. *Peptides Chemistry, Structure, and Biology*; Rivier, J. E., Marshall, G. R., Eds.; ESCOM: Leiden, 1990; pp 575–577. Ghadiri, M. R.; Choi, C. *J. Am. Chem. Soc.* **1990**, *112*, 1630–1633.

(11) Presta, L. G.; Rose, G. D. *Science* **1988**, *240*, 1632. Richardson, J. S.; Richardson, D. C. *Science* **1988**, *240*, 1648.

(12) Ramachandran, G. N.; Sasisekharan, B. *Adv. Protein Chem.* **1968**, *23*, 283.

(13) Nemethy, G.; Phillips, S. C.; Leach, S. J.; Scheraga, H. A. *Nature* **1967**, *214*, 363.

(14) Karle, I. L. *Biopolymers* **1989**, *28*, 1–14. Karle, I. L.; Flippen-Anderson, J. L.; Sukumar, M.; Balaram, P. *Int. J. Pept. Protein Chem.* **1988**, *31*, 567–576.

(15) Arrhenius, T.; Lerner, R. A.; Satterthwait, A. C. *UCLA Symp. Mol. Cell. Biol. New Ser.* **1987**, *69*, 453.

(16) Kemp, D. S.; Rothmann, J.; Curran, T. P. Submitted for publication.

(17) Venkatachalpathi, Y. V.; Balaram, P. *Nature* **1979**, *281*, 83.

(18) Kemp, D. S.; Curran, T. P. *Tetrahedron Lett.* **1988**, *29*, 4931.

(19) Eswarakrishnan, V.; Field, L. *J. Org. Chem.* **1981**, *46*, 4182.

Scheme I[a]

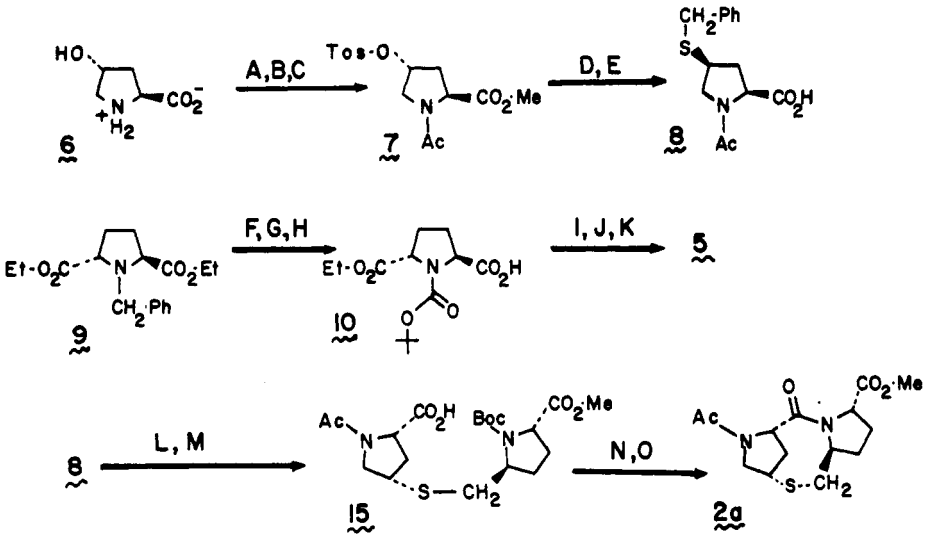

[a] Key: A, MeOH, HCl, $(MeO)_2SO$, 45 °C, 25 h, 93%; B, Ac_2O, H_2O, $NaHCO_3$ 78%; C, Tos-Cl, pyridine, 64%; D, MeOH, NaOH, 82%; E, $PhCH_2$-SNa, DMSO, 78%; F, H_2-Pd/C, EtOH, 50 psi, 40 °C, 18 h, 91%; G, $(Boc)_2O$, MeCN, 2.5 d, 25 °C, 90%; H MeOH, NaOH, 20 h, 23 °C, 63%; I $LiBH_4$, THF, 0 °C, 1.5 h, 23 °C, 13 h, 70%; J, CH_2N_2, THF-MeOH, 89%; K, Tos-Cl, pyridine, 83%; L, NH_3, Na, −78 °C, evaporation; M, DMSO, 5, 23 °C, 14 h, 93%; N, HONp, DCCI, EtOAc, 0 → 23 °C, 4 h, 82%; O, CF_3CO_2H, then 0.001 M in pyridine, DMPA, 113 °C, 20 h, 30%.

Fischer esterification and reversing saponification and displacement steps to circumvent ester epimerization during thioether formation. The overall yield from L-hydroxyproline **6** is 30%, and the sequence can be carried out on a decimolar scale without chromatographic separations. The final step in the formation of (*S,S*)-**4** from **8** involves reductive cleavage of the benzyl function, which is conveniently carried out immediately before reaction with (*S,S*)-**5**, since **4** is not stable to storage, as noted previously.[19]

An obvious precursor of (*S,S*)-**5** is the corresponding *trans*-hydroxymethyl derivative. As reported elsewhere, we considered a stereospecific synthesis of this substance by alkylation of the salt of a [(benzyloxycarbonyl)-amino]malonic ester with (*R*)-4-iodo-1,2-epoxybutane followed by decarboxylation, but obtained only the undesired cis isomer or a cis,trans mixture under a variety of decarboxylation conditions.[20] An alternative route involves resolution and selective reduction of derivatives of *trans*-2,5-dicarboxypyrrolidine, which is readily available in several high-yield steps from the reaction of benzylamine with diesters of 2,5-dibromoadipate.[21] Elsewhere, we have reported a convenient preparation of the key intermediate 1-(*tert*-butoxycarbonyl)-*trans*-2,5-bis(ethoxycarbonyl)-pyrrolidine, the immediate precursor of **10**, as well as anomalous properties of compounds in this series.[22]

For our initial experiments we generated (−)-(*S,S*)-1-benzyl-2,5-dicarboxypyrrolidine in 17% yield from the racemate by (+)-ephedrine resolution following a procedure submitted to us by Katsuki.[23] Fischer esterification of this diacid, followed by hydrogenolysis, reaction with di-*tert*-butyl dicarbonate as previously described,[22] and saponification formed (*S,S*)-**10** in a yield of 47%. The reactions of Scheme I generated (*S,S*)-**5** uneventfully from (*S,S*)-**10** in a yield of 32%. An equivalent route was used to generate racemic *trans*-**5**.

Scheme II[a]

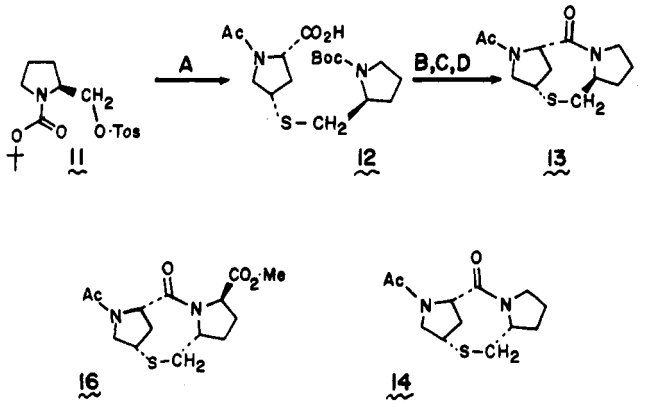

[a] Key: A, **4**, DMSO, 18 h, 23 °C, 94%; B, HONp, DCCI, EtOAc, 0 → 23 °C, 15 h, 32%; C, CF_3CO_2H, 30 min, 0 °C; D, pyridine, 85 °C, 3 days, 32%.

The lactam ring of the target molecule **2** is substantially strained by transannular van der Waals interactions, and while it was expected that this feature would enhance the helix-nucleating properties of the structure by restricting its conformations, it was also expected to complicate the synthesis, since the preparation of strained, peptide-derived lactams often requires high-dilution conditions and a great deal of optimization of experimental conditions. Our first experiments with synthesis of this hitherto unknown tricyclic ring system were therefore directed toward preparation of the model compound **13** and its diastereomer **14** for which precursors were readily accessible by short synthetic routes, as noted in Scheme II.

Following literature procedures, we converted Boc-L-Pro-OH in two steps to (*S*)-1-(*tert*-butoxycarbonyl)-2-[(tosyloxy)methylene]pyrrolidine (*S*)-**11**, obtained as an unstable oil. Debenzylation of **8** with sodium metal in ammonia to form **4**, followed by reaction with **11**, yielded the thioether **12** in nearly quantitative yield. Cleavage of the Boc group of **12** was followed by attempts to achieve cyclization under a variety of conditions (diphenyl phosphorazidate; carbodiimides with and without additives)

(20) Kemp, D. S.; Curran, T. P. *J. Org. Chem.* **1986**, *51*, 2377.
(21) Lowe, G.; Ridley, D. D. *J. Chem. Soc., Perkin Trans. 1* **1973**, 2024.
(22) Kemp, D. S.; Curran, T. P. *J. Org. Chem.* **1988**, *53*, 5729.
(23) Personal communication from Dr. T. Katsuki. See also: Kawanami, Y.; Ito, Y.; Kitagawa, T.; Taniguchi, Y.; Katsuki, T.; Tamaguchi, M. *Tetrahedron Lett.* **1984**, *25*, 857.

that uniformly failed to generate the desired lactam. Conversion of **12** to its *N*-hydroxysuccinimide ester, followed by Boc removal and attempted high dilution cyclization in pyridine of the resulting active ester salt, was similarly unsuccessful.

Conversion of **12** to the *p*-nitrophenyl (ONp) ester was achieved by reaction with dicyclohexylcarbodiimide (DCCI) and *p*-nitrophenol. When this active ester was subjected to trifluoroacetic acid cleavage of the urethane, followed by high dilution cyclization in pyridine at 80 °C, the desired lactam **13** was obtained in 32% yield, characterized by its high-resolution mass spectrum and by its proton NMR spectrum. The corresponding reaction sequence from **4** and (*R,S*)-**11** yielded a separable mixture of **13** and its diastereomer **14**.

The analogous synthesis of **2a** (X = OMe) was initiated by formation of the thioether **15** by reaction of **4** with (*S,S*)-**5** as shown in Scheme I. Conversion to the *p*-nitrophenyl ester, followed by TFA cleavage of the Boc group, generated the amine salt, which was carefully dried then used immediately in the cyclization reaction. In contrast to the ready conversion of the *p*-nitrophenyl ester of **12** to **13**, no conversion of the inductively more deactivated amino ester derived from **15** to **2a** was observed unless the acyl transfer catalyst 4-(dimethylamino)pyridine was present. When the active ester amine salt was added continuously by syringe drive to dry pyridine containing DMAP at 113 °C over 12 h, **2a** was obtained in moderate yield. The structure of **2a** was established by ^{1}H NMR, high-resolution MS, and, as noted in the next section, X-ray crystallography of **2b**. The most practical synthesis of **2a** utilizes the more readily available racemate (*R,R* + *S,S*)-**5**, and from it the above reaction sequence generates **2a** and its diastereomer **16** in a cyclization yield of 58%. The mixture of **2a** and **16** is readily separable chromatographically. Although demethylation of **2a** could also be carried out by reaction with LiI in dioxane, the most convenient preparation of the acid **2b** is achieved by simple saponification, which proceeds in 75% yield. The above synthetic route has proved to be reproducible, and more than 2 g of methyl ester **2a** have been generated by batchwise synthesis following this protocol.

Both **2a** and **2b** show exceptional aqueous solubility. Either substance is easily lost to aqueous phases during extractive workups, and **2b** is nearly insoluble in relatively nonpolar organic solvents. This is an unusual property for an organic molecule that lacks donor hydrogen-bonding sites or internal charges, and we attribute it to the alignment of amide dipoles that is discussed in the following sections.

X-ray Structural Analysis of 2b

Although its derivatives have thus far defied attempts at crystallization, the acid **2b** forms large, well-formed prisms when a saturated solution in water is allowed to stand for a few hours at 23 °C. X-ray structural analysis was carried out, yielding the structure shown in the Ortep projection of Figure 1, which confirms the expected configuration in all respects.

Several structural features are noteworthy. The acetamido function has the s-cis conformation, incapable of helix nucleation. Moreover, the torsional angles SC_9,C_8N_4 and SC_9,C_8C_7 at the C_8–C_9 carbon–carbon single bond have values of 29.5° and 143.8°, respectively. An eclipsed orientation, which is most favorable for helix nucleation, would have torsional values at these torsional angles of 0° and 120°, respectively, while a pure staggered orientation would have values of 60° and 180°. The observed orientation at the C_8–C_9 bond is thus almost exactly the mean

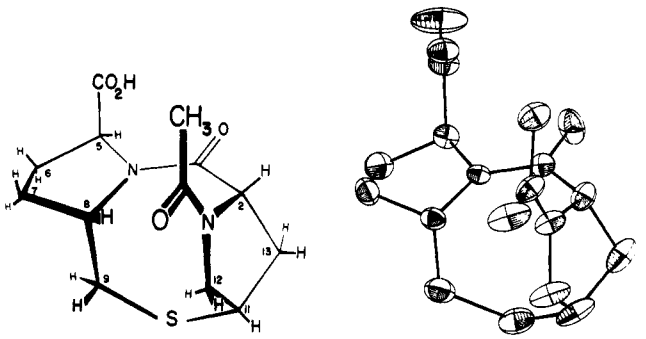

Figure 1. An ORTEP projection of the structure in the crystal of **2b** is shown on the right, as established by X-ray structural analysis. For comparison, a standard structural diagram appears on the left.

of the staggered and eclipsed geometries. The torsional angle $C_{12}C_{11},SC_9$, which defines one of the two junctions between the first pyrrolidine ring and the thialactam ring, is only 11.5°, implying a nearly eclipsed orientation at this site. As a consequence, even if the acetamido function had the s-trans orientation, its carbonyl bond would lie 5–10° off the helical axis determined by the other amide functions. This deviation can also be examined by comparing the observed (ϕ,ψ) angle pairs of (−81.0°, −20.0°) and (−67.4°, −28.8°) of **21** in the crystal with the values of (−65 ± 6°, −41 ± 6°) observed for α-helices in protein structures.[24]

The ring strain of the lactam function is manifested in substantial increases in the bond angles that span the eight-membered ring. Thus, the thioether angle C_9SC_{11} is 109.0° (104° expected), the amide bond angle $C_2C_3N_4$ is 124.2° (115.6° expected), the angle $C_3N_4C_8$ at the lactam nitrogen is 131.1° (119.5° expected), and the following angles at tetrahedron carbon atoms, which are expected to lie close to 109.5°, are all increased substantially above that value: $C_{13}C_{11}S$, 117.3°; $N_1C_2C_3$, 117.8°; $N_4C_8C_9$, 113.9°; C_8C_9S, 119.9°.

Conformational Analysis of the *N*-Methylamide 2c by Molecular Mechanics Modeling

A conformational analysis of **2c** was carried out using the Karplus CHARMm minimization program[25] as implemented in the QUANTA molecular mechanics software package marketed by Polygen Corp. Burst dynamics generation of random structures followed by energy minimization of each established that **2c** has 16 low-energy conformations, although conformations of higher energy, for example, involving formation of a trans lactam function, were occasionally encountered. These principal conformations result from variation of local structure at four sites: the acetamido function, which can assume s-cis (c) or s-trans (t) conformations; the thialactam ring, which can assume eclipsed (e) or near-staggered (s) conformations at the C_8–C_9 bond; the C-5 acyl function, the torsional angle N_4C_5,CO of which can assume values of ca. −25° (α) or +90° (γ); and the C-5 pyrrolidine ring, which can assume a pucker toward (1) or away from (2) the convex side of the molecule. The conformation of the C-2 pyrrolidine ring appears to be locked, as evidenced by a near-superimposability of its atoms in essentially all of the energy-minimized conformations.

The 16 significant conformations can thus be described by a series of four identifiers, one from each of the pairs

(24) Chothia, C. *Ann. Rev. Biochem.* **1984**, *53*, 537–572.
(25) Brooks, B.; Bruccoleri, R.; Olafson, B.; States, D.; Swaminathan, S.; Karplus, M. *J. Comput. Chem.* **1983**, *1*, 187.

given in the following expression: (c,t)(s,e)(α,γ)(1,2). All of the conformations described by the final identifier 2 were found to be 4–5 kcal/mol higher in energy than the corresponding conformations with the pyrrolidine pucker facing the convex face. Consequently, the eight conformations with identifier 2 were ignored in the following analysis.

Are the (e) and (s) states of the eight-membered ring well-defined, or do they belong to a continuum of nearly isoenergetic rotational orientations at the C8–C9 bond? To address this question, a reaction coordinate for interconversion of (csγ1) and (ceγ1) states was defined by using torsional constraints at the C8–C9 and S10–C11 bonds to construct a series of intermediate geometries, each of which was energy-minimized. Removal of the constraint and calculation of the energy of each structure allowed construction of an energy contour and identification of a transition state at a N4C8,C9S10 torsional angle of 80° with an energy of 3.4 kcal/mol relative to the staggered (csγ1) conformation. The (e) and (s) states therefore are likely to equilibrate very rapidly at ordinary temperatures, but they correspond to well-defined energy minima. Variation of the N4C8,C9S10 torsional angle in the range of 30–50° results in only a modest energy increase (<0.5 kcal/mol), implying that the (s) conformations are relatively flexible. The (e) conformations appear to be considerably more constrained, with an accessible N4C8,C9S10 torsional angle in the range of 108–115°.

Inspection of the eight energy-minimized conformations and comparison of their strain energies with that found for a cognate Ac-Pro-Pro-NHMe structure show that the thialactam ring confers substantial torsional, van der Waals, and bond angle strain on these molecules, which can be estimated at ca. 15–16 kcal/mol. All (s) conformations show close nonbonded interactions between 8-H and 1-N, 8-H and 12-H, and particularly 9-H and 12-H; for the (csγ1) conformation, these distances are, respectively, 2.21, 2.12, and 2.05 Å. All (e) conformations show close nonbonded interactions between 8-1 and 1-N and particularly between 13-H and 9-H; for the (ceγ1) conformation, these distances are, respectively, 2.26 and 1.94 Å.

If one excludes (ceα1), which has atypical nonbonded interactions between the acetyl methyl and methylamide functions, strain energies follow consistent patterns. The torsional strain energies for the (s) conformations fall in the range of 10.9–11.1 kcal/mol and for the (e) conformations in the range of 15.3–15.8 kcal/mol. Angle strain energies for the (s) conformations fall in the range of 23.1–23.6 kcal/mol, and for the (e) conformations, in the range of 18.2–19.0 kcal/mol. Given this energetic consistency, one might expect to find an analogous consistency of structure. Superimpositions of (teα1) on the three other (e) conformations show an average root mean square (rms) deviation of 0.060 Å for the atomic positions of the tricyclic nucleus, and superimpositions of the three other (s) conformations on (csγ1) show an average rms deviation of 0.055 Å for the atoms of the tricyclic nucleus. By contrast, superimposition of the atoms of the tricyclic nuclei of (ceα1) and (csα1) shows an rms deviation of 0.45 Å. Probably because of the high internal strain energy of the tricyclic nucleus, variation of conformation of the side-chain acyl functions thus has an insignificant effect on the conformation of this nucleus, which can be viewed as structurally decoupled from the side chains.

An obvious test of the quality of this energetic analysis is its capacity to predict the geometry of **2b** in the crystal, particularly in the tricyclic nucleus, where internal strain

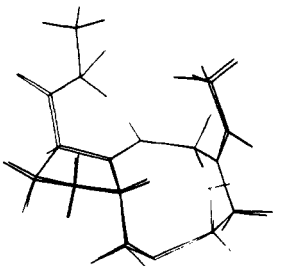

Figure 2. A superimposition of the structure of the acid **2b** in the crystal as established by X-ray diffraction and a conformation (csγ1) of the *N*-methylamide **2c** obtained by a CHARMm energy minimization.

is expected to render the geometry insensitive to crystal packing forces. Figure 2 shows a superimposition of the crystal structure of the acid **2b** on the energy-minimized (csα1) conformation of the methylamide **2c**. The atomic positions of these two structures show an rms deviation of atomic position of only 0.07 Å, and it is striking that both tricyclic and side-chain atoms assume essentially identical geometries in both structures.

Although this agreement is gratifying, it does not imply that molecular mechanics can provide a precise quantitation or even a rank ordering of the relative stabilities of the eight significant conformations of the methylamide **2c**. The nature of the problem is evident if one sums torsional and angle strain energies, which together with the electronic energy are the major contributors to the molecular mechanics energy function for these structures. For the seven cases (again, (ceγ1) was excluded) an average value for this sum is 34.19 ± 0.22 kcal/mol. This constancy implies that to a first approximation effects on relative energies due to torsional and angle strain will cancel, leaving estimates of relative energies largely dependent on differences in electronic energy as well as on sums of small differences in other effects.

Electronic effects are calculated in CHARMm by assigning partial atomic charges to every atom and summing the resulting electrostatic interactions. Electronic effects are strongly influenced by solvent, and as noted in the Experimental Section, several different models for electronic and solvation effects were used to calculate the relative energies of the eight conformations. All gave results that were in relatively poor agreement with one or the other of the two pertinent experimental findings, discussed in the spectroscopic section: (1) in solvents other than chloroform the energy difference between the most stable of the (ts) conformers and the most stable of the (cs) conformers is 0.3–1.0 kcal/mol, and (2) the most stable (e) conformation is at least 1.0 kcal/mol less stable than the most stable (cs) conformation. The best fits were obtained using standard peptide charge assignments and a constant dielectric model with a dielectric constant of ca. 10 or greater; these gave 0.4–0.8 kcal/mol for the former parameter and −0.5 kcal/mol for the latter.

The energy difference of greatest significance for the use of derivatives of **2** as helix nucleation sites is that between the nucleating conformation (teα) of **2c**, which will be shown in the accompanying paper to be the dominant conformation of helical template–peptide conjugates in relatively nonpolar solvents and the nonnucleating conformation (cs), which is shown here to be the dominant conformation of simple derivatives of **2** in nonpolar solvents. Contrary to experiment, all computational estimates of this difference imply that the (te) conformation should be the more stable, and the best computational estimates of this difference are ca. −0.5 kcal/mol, inconsistent with

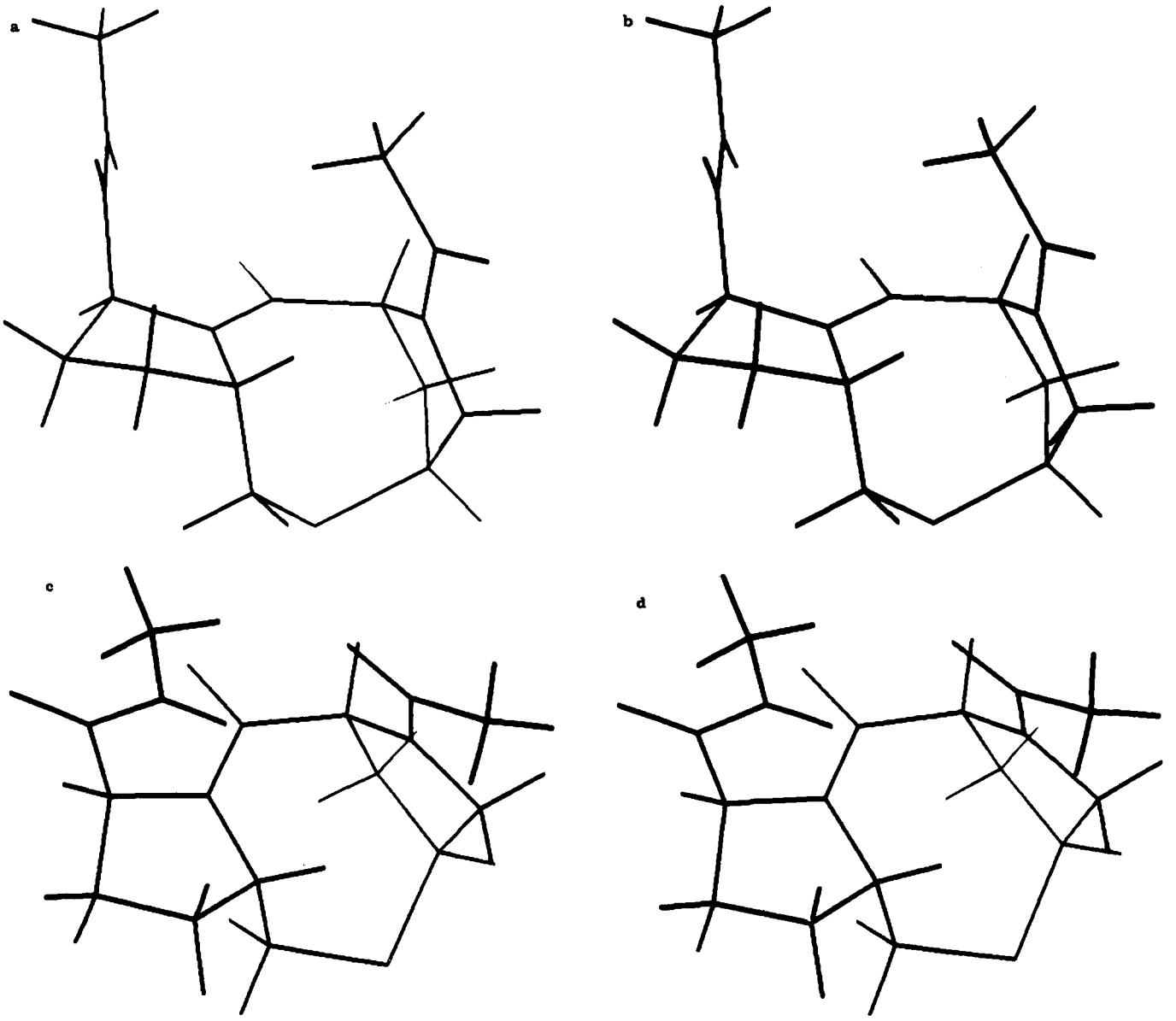

Figure 3. Computer-generated stereograms of the nonnucleating conformation (csγ1) (top) and the nucleating conformation (teγ1) (bottom) of **2c**, obtained by CHARMm minimization.

the greater experimental stability of the (cs) state. Given the uncertainties in the above analysis, these should probably be taken to imply that the enhanced relative stability of the nonnucleating (csγ1) over the helix-nucleating (teα1) cannot be much greater than the experimental lower bound of 1.0 to 1.2 kcal/mol. These relative energies are almost certainly less accurately modeled than their corresponding structures. The computer-generated stereodiagrams of Figure 3 depict the energy-minimized conformations of two structural archetypes: the helix-nucleating conformation (teα1) and the nonnucleating conformation (csγ1). These are probably realistic depictions of the actual molecular conformations.

Solution Conformations of 2a and 2b

The ^{1}H NMR spectra were obtained and analyzed to determine the experimentally observed conformations of **2a** in $CDCl_3$, CD_3CN, DMF-d_7, and DMSO-d_6 and **2b** in D_2O. From the standpoint of polarity, chloroform and water are the limiting solvents in this series, and the ^{1}H NMR spectra in these solvents are shown for comparison in Figure 4. With the exception of the region of δ 1.9–2.3, which contains overlapping peaks corresponding to the C-9a, C-7, and C-6 proton resonances, and the region of δ 3.55–3.85, which contains the C-11 and C-12 proton resonances, all peaks are well separated in all solvents studied. Table I reports chemical shift values and spin multiplicities for these two spectra, along with the positional assignments that are the result of COSY analyses. In all solvents other than chloroform, each type of hydrogen is represented as a pair of resonances resulting from s-cis/s-trans rotational isomerization of the acetamide function that is slow on the NMR time scale under the experimental conditions.

Nuclear Overhauser effects (NOEs) in $CDCl_3$ solution were used to establish the orientation of the acetamido function of **2a**, the conformation of the lactam ring, and the chemical shift assignments of protons 9a and 9b; NOEs of **2b** in D_2O, in which two slowly equilibrating conformational subspecies are present, permitted analogous assignments in this solvent for both subspecies. For **2a** in $CDCl_3$, strong reciprocal NOEs were observed between resonances of the acetyl methyl and the C-2 protons, but no NOE interaction could be detected between resonances of the acetyl and the C-12 protons. The acetamide in this solvent therefore assumes the s-cis orientation, and the

Table I. Chemical Shift Assignments for 2a and 2b at 25 °C

2a in $CDCl_3$ (500 MHz)			2b in D_2O pD 1.6 (500 MHz)[a]		
δ (ppm)	coupling pattern, J (Hz)	assignment	δ (ppm)	coupling pattern J (Hz)	assignment
4.67	d, 8.7	2-H	4.79	d, 9.2	2-H[a]
			4.76	d, 9.6	2-H'[a]
4.65	d, 8.5	5-H	4.57	d, 8.8	5-H
			4.46	d, 9.5	5-H'
4.38	m	8-H	4.36	m	8-H'
			4.31	m	8-H
3.83	m	12a-H, 12b-H	4.00	dd, 5.9, 12.5	12a,b-H'
			3.83	m	12a,b-H
3.74	s	OCH_3			
3.61	33, 5.4, 5.6	11-H	3.77	m	11-H,H'
3.18	dd 5.1, 15	9b-H	3.33	dd, 5.9, 14.3	9b-H,H'
2.78	m	13b-H	2.86	m	13b-H
			2.74	m	13b-H'
2.58	d, 14	13a-H	2.56	dd, 9.1, 15.7	9a-H'
			2.50	dd, 10.3, 15.3	9a-H
2.32	dd, 9.9, 15	9a-H	2.47	d, 13.5	13a-H
			2.37	d, 14.0	13a-H'
2.30	m	7b-H	2.24	m	7b-H,H'
			2.24	m	6b-H,H'
2.20	s	Ac	2.14	2s	Ac,Ac'
2.11	m	6b-H			
1.96	dd, 6, 13	6a-H	2.03	m	6a-H,H'
1.70	dd, 6, 13	7a-H	1.91	m	7a-H,H'

[a] A prime (') designates a resonance belonging to the s-trans conformation as established by COSY and ROESY experiments. The c/t ratio is 3:2. The peak positions in D_2O are relative to 1.00 = trimethylsilanepropionic acid.

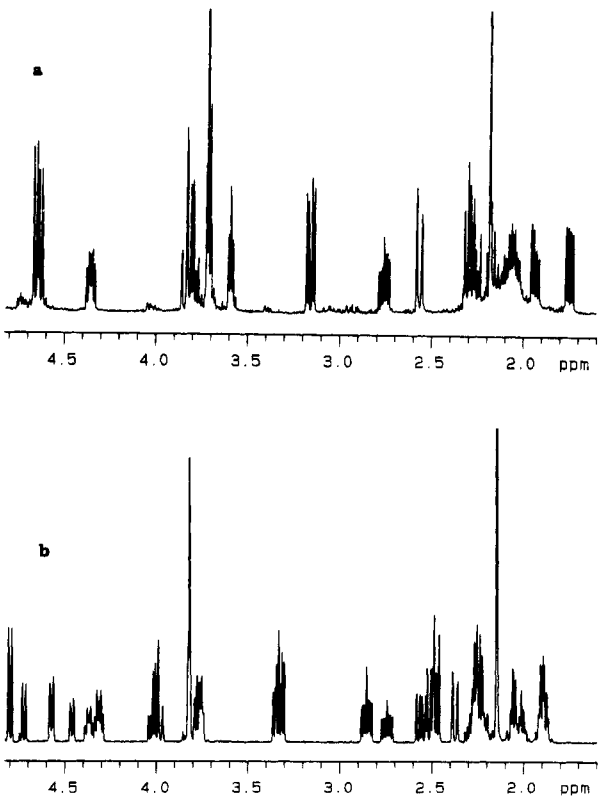

Figure 4. (a) ^1H NMR spectrum of the methyl ester **2a** in $CDCl_3$, 300 MHz, 23 °C. (b) ^1H NMR spectrum of the acid **2b** in D_2O, 500 MHz, pH 0.8, 23 °C. Owing to overlap with a DHO resonance, the C-2 and C-2' resonances are not shown. The peak assignments for these spectra are reported in Table I. (The resonances for CO_2CH_3 and $COCH_3$ have been truncated.)

absence of resonances that would be expected if the slowly equilibrating s-trans amide conformers were present establishes that in $CDCl_3$ >98–99% of the molecules are in this (c) state.

In the D_2O spectrum of **2b** at pH 0.8 all resonances except those for the proton at C-2 (partially obscured by the DHO peak) and those at C-6, acetyl, and C-7 (overlapping) appear as cleanly resolved pairs of peaks with an area ratio of 3:2. With the exception of resonances assigned to the pair of methylene protons at C-12, which are distinguishable in δ values for the 12ab protons owing to changes in carbonyl anisotropy, each pair of resonances exhibits the same peak pattern and essentially the same coupling constants. A ROESY analysis confirmed that the major and minor peaks belong to separate, noninteracting spin systems of separate molecules and demonstrated significant NOE effects between the major C-2 resonance (δ 4.79) and the acetyl, which appears as an unresolved doublet, as well as between the minor C-12 resonance (δ 4.00) and the acetyl. These interactions were confirmed by classical NOE irradiation experiments. The major peaks therefore belong to a (c) conformation of **2b**, the minor peaks belong to a (t) conformation, and these are present in a 3:2 ratio. In D_2O at pH 5, the anion of **2b** shows a similar NMR spectrum, but with a c/t area ratio of 2:1. (Use of the carbonyl anisotropy-induced chemical shift difference for the C-12 proton resonances to assign c/t conformations was avoided since the orientation lies close to the region of sign reversal[26] and reversal of the sign of anisotropy with solvent change has been reported.[27])

Spectra of **2a** in CD_3CN, DMF-d_7, and DMSO-d_6 are similar to the water spectrum of **2b**. If one assumes that the major peaks in all these solvents are attributable to the (c) conformation, then the c/t ratios are as follows: $CDCl_3$ >30; CD_3CN, ca. 5:1; DMF-d_7, 3:1; DMSO-d_6, 3:1; D_2O, 1.5:1. The increase in relative stability of the (c) conformation as the solvent polarity is reduced doubtless reflects the increasing difficulty in aligning three dipoles. A similar trend of c/t ratios is seen for the structure **12**, which lacks one of the destabilizing carbonyl dipoles: $CDCl_3$, 4:1; CD_3CN, 1:1; DMF-d_7, 0.7:1; DMSO-d_6, 0.7:1; D_2O, 0.5:1.

NMR spectroscopic data in the form of chemical shift differences, NOE interactions, and J values also define the conformation of the thialactam ring in D_2O. As noted in

(26) Paulsen, H.; Todt, K. *Chem. Ber.* **1967**, *100*, 3385.
(27) Deber, C. M.; Bovey, F. A.; Carver, J. P.; Blout, E. R. *J. Am. Chem. Soc.* **1970**, *92*, 6191.

the structures of Figure 3, conversion of the (s) to the (e) state results in substantial changes in torsional angles and in the magnetic environment of specific protons. Strikingly, only small changes in chemical shift and no significant changes in coupling constant are observed for **2a** and **2b** when the solvent is varied through the series $CDCl_3$, CD_3CN, DMF-d_7, DMSO-d_6, and D_2O. Thus the pair of methylene protons at C-9 shows chemical shift differences of δ 0.86, 0.83, 0.73, 0.75, and 0.79 in this solvent series, and the vicinal $J_{8\text{-}H,9\text{-}H}$ values are consistently 5.5 ± 0.2 and 9.9 ± 0.2 Hz. Similarly, interconversion between the (c) and (t) states results in only a modest change in chemical shifts and essentially no change in coupling constants, as can be seen in the D_2O spectrum of Figure 4. Rapid equilibration between (e) and (s) conformations of roughly equal energy is expected to result in an averaging of chemical shifts and coupling constants for the diastereotopic hydrogens at C-9. Moreover, solvent effects on the relative stability of these conformations would be expected to result in detectable changes in coupling constants and chemical shifts. The observed invariance of these properties is thus consistent with a dominant conformation for the thialactam ring and the tricyclic framework.

In the molecular mechanics model the (s) states are characterized by a 2.05-Å nonbonded separation between protons at C-12 and C-9b of **1**, in contrast to the (e) states, which have a 1.94-Å separation between protons at C-13 and C-9a. Irradiation of the C-12 resonance in the $CDCl_3$ spectrum of **2a** results in strong NOE signals at δ 4.38 (C-8), 3.61 (C-11), and 3.18 (C-9). Irradiation of the δ 3.18 C-9 resonance results in NOE signals at δ 4.38, 2.32, and 3.83, corresponding to protons at C-8, C-9, and C-12. A ROESY analysis of **2b** in D_2O demonstrated an NOE effect between the δ 3.83 and 3.33 resonances, which correspond to the C-12 and C-9 protons of the dominant (c) conformation. No NOE interactions could be detected between the C-9 and C-13 protons in $CDCl_3$ or D_2O. The dominant conformation of the thialactam is therefore the (s) state, and the resonances at δ 3.16–3.18 and 2.32–2.39 must be assigned to protons at C-9b and C9a, respectively.

Independent evidence in support of this assignment is available from consideration of the conformational environment at the C-8,C-9 single bond. As noted above, the (s) states are characterized by dihedral angles H C-8,C-9,H-9b of 30–50° and H C-8,C-9,H-9a of 150–170°, which should result in coupling constants similar to the $J_{ax,eq}$ (2–6 Hz) and $J_{ax,ax}$ (8–13 Hz) values observed with substituted cyclohexane derivatives and sugar derivatives.[28] The corresponding angles for the (e) states are 110–115° and 130–125°, which should result in a pair of J values that are small and similar in magnitude. Although the large chemical shift differences render this a simply analyzable AMX spin system, quantitative calculation of dihedral angles through application of the Karplus equation to the resulting $J_{H\text{-}8,H\text{-}9}$ values is problematic, given the presence in the system of electronegative atoms as well as substantial angle strain.[28,29] However, the analogy to chair conformations of six-membered rings appears appropriate, and the observation of a $J_{H\text{-}8,H\text{-}9b}$ value of 5.5 Hz and a $J_{H\text{-}8,H\text{-}9a}$ value of 10 Hz by that analogy confirms the assignment of the (s) state to the thialactam. In the accompanying paper it is shown that peptide conjugates of **2** that assume helical conformations are characterized by dramatic chemical shift changes for resonances attributable to protons at C-9 and C-13, as well as by changes in both the $J_{H\text{-}8,H\text{-}9b}$ value (5.5 to 2.3 Hz) and the $J_{H\text{-}8,H\text{-}9a}$ value (9.9 to 4.5 Hz). The new J values seen for helical template–peptide conjugates are thus consistent with a conformational change to the thialactam (e) state.

The simple acyl derivatives of **2** exhibit an invariance of both $J_{H\text{-}8,H\text{-}9}$ values with solvent and c/t conformational changes that is consistent with a single dominant thialactam conformation, rather than an environment-dependent dynamic average of two contributing conformations. The large changes in J and δ values for the C-9 proton resonances with peptide conjugation and the correspondingly dramatic changes in NOE signatures for the C-9 resonances also support this conclusion.

Summary

A practical synthesis is described for a tricyclic helical template, derived from acetyl-L-prolyl-L-proline by introducing a thiomethylene bridge as a conformational constraint. X-ray analysis of a crystal of **2b** as well as solution ^1H NMR studies of **2b** and its methyl ester **2a** establish that the thialactam ring in these derivatives assumes a staggered (s) conformation unfavorable for helical nucleation. In chloroform, only the nonnucleating s-cis (c) acetamido conformation can be detected. In more polar solvents including water, a mixture of (c) and (t) states is detected. In accord with these solution studies, the preferred geometry of **2b** in the crystal is shown to be the helix nonnucleating (cs) conformation. Of the four possible combinations of geometry at the acetamide function and the thialactam, only two, the (cs) and the (ts) geometries, have been seen in solution for simple acyl derivatives of **2**. A molecular mechanics analysis of the conformations of the methylamide **2c**, though inconsistent with the relative conformational energetics of **2ab** in solution, is in accord with all other experimental findings.

Experimental Section

Anhydrous pyridine was fractionally distilled from NaOH through a Vigreux column; the first tenth of the distillate was discarded, and the center fraction was stored over freshly activated 3-Å sieves. DMF was distilled from ninhydrin and stored over sieves. Triethylamine was distilled from CaH_2 and stored over sieves. Diisopropylethylamine was distilled from ninhydrin, then from NaOH/Na, then stored over sieves. Tetrahydrofuran (THF) and dioxane were freshly fractionated from sodium/benzophenone ketyl. Reagent-grade CH_2Cl_2 (DCM), $CHCl_3$, DMSO, benzene, pyridine, and MeCN were stored over freshly activated 3-Å sieves. Sequanal-grade trifluoroacetic acid (TFA) was obtained from Pierce Chemical and was stored in a desiccator when not in use. Tosyl chloride was used as received from a freshly opened bottle. Diazomethane was prepared in ether solution from diazald and used immediately.

Analytical TLC was performed on E. Merck 0.25-mm F-254 silica gel 60 plates with glass backing. Flash chromatography was performed using E. Merck silica gel 69 (230–400 mesh).

1-Acetyl-2(*S*)-carboxy-4(*S*)-(benzylthio)pyrrolidine (8). A. Methyl *trans*-4-Hydroxy-L-prolinate Hydrochloride. Thionyl chloride (50 mL, 0.69 mol) was added to methanol (250 mL) at 0 °C, and to the resulting mixture at 23 °C was added 4-*trans*-L-hydroxyproline. The mixture was heated and stirred at 45 °C for 16 h and then concentrated to a solid that was treated with ether (3 × 50 mL) followed by evaporation. Recrystallization of the solid from MeOH–ether gave 64.6 g (93%) of **6** in two crops, mp 171–172 °C (lit.[19] mp 171–172 °C).

B. Methyl *N*-Acetyl-*trans*-4-hydroxy-L-prolinate. To a stirred solution of **6** (64.6 g, 0.36 mol) in dioxane–H_2O (1:1, 200 mL) at 0 °C was added $NaHCO_3$ (62.8 g, 0.75 mol) in small portions over 10 min, together with acetic anhydride (37 mL, 0.39 mol), dropwise over 30 min. After 2 h at 23 °C, the resulting solution was concentrated, diluted with H_2O (100 mL) and sat-

(28) Jackman, L. M.; Sternhell, S. *Applications of Nuclear Magnetic Resonance Spectroscopy in Organic Chemistry*, 2nd ed.; Pergamon Press: Oxford, 1969; p 288. Abraham, R. J.; Fisher, J.; Loftus, P. *Introduction to NMR Spectroscopy*; Wiley-Interscience: Chichester, 1988; pp 44–45.
(29) Karplus, M. *J. Am. Chem. Soc.* **1963**, *85*, 2870.
(30) Patchett, A. J.; Witkop, B. *J. Am. Chem. Soc.* **1957**, *79*, 185.

urated with NaCl, and extracted with $CHCl_3$ (10 × 100 mL). The pooled extracts were dried, filtered, and concentrated to a solid that was recrystallized from EtOAc–ether to yield 51.9 g (78%), mp 80–81 °C (lit.[19] mp 78 °C).

C. Methyl *N*-Acetyl-*trans*-4-(tosyloxy)-L-prolinate (7) and *N*-Acetyl-*trans*-4-(tosyloxy)-L-proline. To a solution of *p*-toluenesulfonyl chloride (12.5 g, 65.8 mmol) in pyridine (25 mL) in a flame-dried flask was added at 0 °C with stirring methyl *N*-acetyl-*trans*-4-hydroxy-L-prolinate (11.2 g, 59.8 mmol). After 15 h at 0 °C, the mixture was poured into 1 M HCl (180 mL), and the solution was extracted with EtOAc (3 × 60 mL). The pooled extracts were washed with 1 M HCl (3 × 30 mL), saturated $NaHCO_3$ (2 × 30 mL), and brine (2 × 30 mL) and then were dried and concentrated to a tan oil that was crystallized from ether to yield 7, 11.3 g (64%), mp 70–72 °C (lit.[19] mp 71–73 °C). To a stirred solution of ester (11.4 g, 33.4 mmol) in methanol (85 mL) at 0 °C was added 1 M NaOH (35 mL, 35 mmol); the mixture was slowly warmed to 23 °C and then rechilled to 0 °C and treated with 1 M HCl (35 mL). After 15 min, a white solid was collected by filtration, dried, and recrystallized from acetone–ether to yield the acid, 9.5 g (82%), mp 183–184 °C (lit.[31] mp 182–182 °C).

D. *N*-Acetyl-*cis*-4-(benzylthio)-L-proline (1-Acetyl-2-(*S*)-carboxy-4(*S*)-(benzylthio)pyrrolidine) (8). To a solution obtained from sodium metal (7.25 g, 0.32 mol) in dry EtOH (200 mL) in a flame-dried flask was added benzyl mercaptan (35.1 mL, 0.30 mmol), and the solvent was evaporated at 30 °C. The white residue was dissolved in DMSO (125 mL) to which *N*-acetyl-*trans*-4-(tosyloxy)-L-proline (49.0 g, 0.15 mol) was then added with stirring. After 16 h, the solvent was evaporated, and the residue was dissolved in H_2O (400 mL). The solution was washed with ether (3 × 100 mL) and then acidified to pH 1 (HCl) and extracted with $CHCl_3$ (3 × 100 mL). The pooled extracts were washed (1 M HCl, 50 mL), dried, and concentrated to yield an oil that was crystallized from $CHCl_3$–ether to yield 8, 32.6 g (78%), mp 138–140 °C (lit.[19] mp 140–141 °C).

Racemic *trans*-1-(*tert*-Butoxycarbonyl)-2-(methoxycarbonyl)-5-[(tosyloxy)methyl]pyrrolidine ((*R*,*R* + *S*,*S*)-5) and *trans*-1-(*tert*-Butoxycarbonyl)-2(*S*)-(methoxycarbonyl)-5(*S*)-[(tosyloxy)methyl]pyrrolidine ((*S*,*S*)-5). A. Racemic *trans*-1-(*tert*-Butoxycarbonyl)-2-(methoxycarbonyl)-5-[(tosyloxy)methyl]pyrrolidine ((*R*,*R* + *S*,*S*)-5). (The spectroscopic properties for the intermediates in this series were identical with those reported subsequently for the enantiomeric series.)

To a solution of *trans*-1-(*tert*-butoxycarbonyl)-2,5-bis(ethoxycarbonyl)pyrrolidine prepared as previously reported[20] (19.3 g, 61.2 mmol, 1.0 equiv) in ethanol (90 mL) was added dropwise over 90 min aqueous NaOH (67 mL, 1.0 M) at 23 °C with stirring. After 3 d, the solvent was evaporated, the residue was dissolved in water (100 mL), and the solution was washed (ether, 3 × 50 mL), acidified to pH 2 (1 M HCl), and extracted (ether, 3 × 75 mL). Pooling of the extracts, drying, and evaporation and drying at high vacuum yielded *trans*-1-(*tert*-butoxycarbonyl)-2-carboxy-5-(ethoxycarbonyl)pyrrolidine (10; 13.0 g, 74%) as an oil.

In a flame-dried flask was treated dropwise with stirring a solution of $LiBH_4$ (186 mmol, 4.1 equiv) in freshly distilled THF (75 mL) at 0 °C over 20 min with the above-prepared oil (13.0 g, 45.1 mmol, 1.0 equiv) in THF (150 mL). After 1 h at 0 °C and 12 h at 23 °C the solution was rechilled and carefully treated with H_2O (25 mL, 30 min). The solution was diluted with water–ether (600 mL, 5:1), and the separated H_2O phase was washed (ether 2 × 100 mL) and then acidified to pH 2, saturated with NaCl, and extracted (EtOAc 4 × 100 mL). The combined extracts were dried and evaporated. After 20 h in vacuum, the resulting oil (8.61 g, 78%) was dissolved in THF (200 mL) and treated with excess CH_2N_2 in ether. After treatment with HOAc, the solvent was evaporated, the residue was dissolved in ether (150 mL), and the solution was washed (3 × 25 mL of saturated $NaHCO_3$; 25 mL of brine), dried, and evaporated to yield 8.76 g of the racemic methoxycarbonyl hydroxymethyl derivative.

A solution of 17.7 g (68.4 mmol, 1.0 equiv) of this substance in dry pyridine (70 mL) was added with stirring at 0 °C to *p*-toluenesulfonyl chloride (14.3 g, 75.0 mmol) in pyridine (35 mL). After 18 h at 0 °C the solution was poured into ice (300 mL) and 12 M HCl (100 mL), and the resulting mixture was extracted with EtOAc (4 × 100 mL). The pooled extracts were washed (0.25 M HCl, 3 × 50 mL; saturated $NaHCO_3$, 3 × 50 mL; brine, 50 mL), dried, and evaporated to yield 25.1 g (89%) of the title compound, (*R*,*R* + *S*,*S*)-5, as a white solid, which can be recrystallized from EtOAc–hexane, mp 116–118 °C. Anal. Calcd for $C_{19}H_{27}NO_7S$: C, 55.19; H, 6.58; N, 3.39. Found: C, 54.80; H, 6.51; N, 3.38.

B. *trans*-1-(*tert*-Butoxycarbonyl)-2(*S*),5(*S*)-bis(methoxycarbonyl)pyrrolidine. A solution in EtOH (300 mL) of racemic *trans*-1-benzyl-2,5-bis(ethoxycarbonyl)pyrrolidine (92.0 g, 0.301 mol, 1.0 equiv), prepared from diethyl 2,5-dibromoadipate as previously described,[20] was treated with NaOH (30.1 g, 0.75 mol, 2.5 equiv) in 450 mL of H_2O. After 8 h at 23 °C the solvent was evaporated and the residue was added with stirring to HCl (5 M, 134 mL) at 0 °C for 5 h, and then was collected, washed, and recrystallized (H_2O) to yield racemic *trans*-1-benzyl-2,5-dicarboxypyrrolidine as white crystals, 35.4 g (47%), mp 186–189 °C.

A suspension of the above compound (12.0 g, 48.2 mmol, 1.0 equiv) and (+)-ephedrine (7.96 g, 48.2 mmol, 1.0 equiv) in EtOH (5.25 mL) was heated until solids dissolved then cooled slowly to 18 ± 1 °C and stirred for 18 h. The resulting crystals were collected and air-dried to yield a crude salt (5.96 g, 30%) that was recrystallized from MeOH (40 mL) to yield 3.47 g (17%), mp 227–228 °C, $[\alpha]_{589}$ −29.6° (*c* 2.85, MeOH) (lit.[23] −28.3°).

A solution of the above-prepared ephedrine salt (9.95 g, 24.0 mmol, 1.0 equiv) in 0.5 M NaOH (100 mL) was extracted with DCM (2 × 50 mL), acidified (12 M HCl, 4.6 mL), and evaporated. The resulting white solid was added to solution of HCl–dimethyl sulfite, prepared by adding $SOCl_2$ (13 mL) to MeOH (70 mL) at 0 °C. After 4 h of refluxing, the mixture was cooled and evaporated, and the residue was dissolved in half-saturated $NaHCO_3$ (100 mL) to which solid Na_2CO_3 was added to bring the pH to 10. The cloudy solution was extracted with DCM (3 × 60 mL), and the pooled extracts were dried and evaporated to yield, after drying in vacuum, *trans*-1-benzyl-2(*S*),5(*S*)-bis(methoxycarbonyl)pyrrolidine as a clear oil: 6.00 g (90%); $[\alpha]_{589}$ −121° (*c* 2.77, Me_2CO); HRMS calcd for $C_{15}H_{19}NO_4$ 277.13141, found 277.13100.

To a solution in ethanol (60 mL) of the above-prepared compound (6.00 g, 21.7 mmol) was added 10% Pd/C (0.2 g), and the resulting suspension was hydrogenated at 40 °C and 50 psi for 18 h. After cooling and filtration, the solution was evaporated to an oil (3.67 g 91%), which was dissolved in MeCN (4.0 mL) containing *tert*-butyl dicarbonate (4.75 g, 21.8 mmol, 1.1 equiv). After 2.5 d at 23 °C the solvent was evaporated, and the residue was purified by flash chromatography (1:1 ether/hexane) to yield 5.07 g (90%) of the title compound as a white, crystalline solid: mp 71–73 °C; $[\alpha]_{589}$ −71.9° (*c* 1.3 $CHCl_3$); ^1H NMR ($CDCl_3$, 250 MHz) δ 4.54 (1 H, dd, *J* = 1.7, 8.5 Hz), 4.44 (1 H, dd, *J* = 1.7, 8.5 Hz), 3.73 (6 H, s), 2.40–2.22 (2 H, m), 2.10–1.90 (2 H, m), 1.41 (9 H, s). Anal. Calcd for $C_{13}H_{21}NO_6$: C, 54.34; H, 7.37; N, 4.88. Found: C, 54.53; H, 7.17; N, 4.88.

C. *trans*-1-(*tert*-Butoxycarbonyl)-2(*S*)-(methoxycarbonyl)-5(*S*)-[(tosyloxy)methyl]pyrrolidine ((*S*,*S*)-5). (Experimental protocols identical with those reported above for the racemic series were used to form the title compound from *trans*-1-(*tert*-butoxycarbonyl)-2(*S*),5(*S*)-bis(methoxycarbonyl)-pyrrolidine.

1. *trans*-1-(*tert*-Butoxycarbonyl)-2(*S*)-carboxy-5(*S*)-(hydroxymethyl)pyrrolidine. From *trans*-1-(*tert*-butoxycarbonyl)-2(*S*),5(*S*)-bis(methoxycarbonyl)pyrrolidine (4.82 g, 16.8 mmol) was formed by saponification of *trans*-1-(*tert*-butoxycarbonyl)-2(*S*)-carboxy-5(*S*)-(methoxycarbonyl)pyrrolidine (2.89 g, 63%) as a glassy solid, $[\alpha]_{589}$ −120° (*c* 0.37, $CHCl_3$). Reduction of the latter compound (2.79 g, 10.2 mmol) with $LiBH_4$ and subsequent hydrolysis yielded the title compound (1.75 g, 70%) mp 154–156°C: $[\alpha]_{589}$ −80.3° (*c* 1.2, MeOH); ^1H NMR ($CDCl_3$, 300 MHz) δ 4.45–4.30 (1 H, m), 4.28–4.16 (1 H, m), 3.80–3.60 (2 H, m), 3.2 (2 H, br s), 2.40–2.10 (2 H, m), 2.08–1.96 (1 H, m), 1.75–1.65 (1 H, m), 1.50, 1.44 (9 H, 2 s); HRMS calcd for $C_{12}H_{21}NO_5$ 259.14196, found 259.14191.

2. *trans*-1-(*tert*-Butoxycarbonyl)-2(*S*)-(methoxycarbonyl)-5(*S*)-[(tosyloxy)methyl]pyrrolidine ((*S*,*S*)-5). From the hydroxymethyl acid prepared in 1 (1.73 g, 7.06 mmol)

(31) Blarer, S. J.; Seebach, D. *Chem. Ber.* **1983**, *116*, 2250.

by reaction with CH_2N_2 followed by reaction with tosyl chloride in pyridine to form (*S,S*)-**5**, isolated by flash chromatography (7:3 ether/hexane) as a white solid, mp 83–84 °C: $[\alpha]_{589}$ −51.4° (*c* 1.2, $CHCl_3$); ^1H NMR ($CDCl_3$, 300 MHz) δ 7.77 (2 H, dd, *J* = 8.1, 2.9 Hz), 7.34 (2 H, d, *J* = 8.1 Hz), 4.25–4.15 (1 H, m), 4.10–3.90 (1 H, m), 3.70 (3 H, s), 2.44 (3 H, s), 2.45–2.22 (1 H, m, 1.95–1.82 (2 H, m), 1.57, 1.35 (9 H, 2 s): HRMS calcd for $C_{19}H_{27}NO_7S$ minus CO_2CH_3 354.13740, found 354.13752. Anal. Calcd for $C_{19}H_{27}NO_7S$: C, 55.19; H, 6.58; N, 3.39. Found: C, 55.25; H, 6.65; N, 3.43.

(2*S*,5*S*,8*S*,11*S*)-1-Acetyl-1,4-diaza-3-keto-5-(methoxycarbonyl)-10-thiatricyclo[2.8.1.0^{4,8}]tridecane and (2*S*,5*R*,8*R*,11*S*)-1-Acetyl-1,4-diaza-3-keto-5-(methoxycarbonyl)-10-thiatricyclo[2.8.1.0^{4,8}]tridecane (2a). A. Preparation and Separation of a Mixture of the 2*S*,5*S*,8*S*,11*S* and 2*S*,5*S*,8*S*,11*S* Isomers. 1. Thioether Formation. To a suspension at −78 °C of 1-acetyl-2(*S*)-carboxy-4(*S*)-benzylthiopyrrolidine (**8**; 4.72 g, 16.9 mmol, 1.0 equiv) in anhydrous NH_3 (200 mL), contained in a three-necked flask equipped with a Dewar condenser and N_2 inlet, was added Na metal (0.90 g, 39 mmol, 2.1 equiv) in small portions over 2 h. The resulting light blue solution was stirred for 30 min then warmed to 23 °C during evaporation of the NH_3 under a stream of N_2. After 2 h the residual white solid was dissolved in dry DMSO (75 mL) and treated with racemic *trans*-1-(*tert*-butoxycarbonyl)-2-(methoxycarbonyl)-5-[(tosyloxy)methyl]pyrrolidine (*R,R* + *S,S*)-**5** (7.02 g, 16.9 mmol, 1.0 equiv). After 14 h at 23 °C the DMSO was evaporated in vacuum using a cold finger evaporator, the residue was dissolved in H_2O (150 mL) containing 1 M NaOH (5 mL), and the solution was washed (EtOAc 3 × 40 mL). The aqueous phase was carefully acidified to pH 2 (1 M HCl) and extracted (EtOAc 3 × 50 mL). The combined extracts were dried and evaporated to yield the thioether **15** as a foam that was dried in vacuum (6.76 g, 93%) that was used directly in the next preparation: HRMS calcd for $C_{19}H_{30}N_2O_7S$ 430.17735, found 430.17774.

2. *p*-Nitrophenyl Ester Formation and Conversion to 2a. To a solution at 0 °C in EtOAc (12 mL) of the thioether **15** (1.34 g, 3.11 mmol, 1.0 equiv) and 4-nitrophenol (0.434 g, 3.20 mmol, 1.0 equiv) was added dicyclohexylcarbodiimide (720 mg, 3.50 mmol, 1.1 equiv). After 1 h at 0 °C and 3 h at 23 °C the solution was chilled and filtered, and the filtrate was evaporated to yield a yellow oil that was purified by flash chromatography (9:1 EtOAc–hexane) to give 1.41 g (82%) of the diastereomeric *p*-nitrophenyl esters.

To a solution of the *p*-nitrophenyl ester mixture (3.57 mg, 6.48 mmol) in DCM (12 mL) containing anisole (0.2 mL) was added trifluoroacetic acid (15 mL). After 40 min at 0 °C, the solution was evaporated, and the resulting oil was triturated repeatedly with ether then dried in vacuum until a brittle white foam was obtained. This foam was dissolved in freshly distilled dioxane (30 mL) and transferred to an oven-dried 50-mL syringe that was attached by a syringe pump to a flame-dried three-necked flask equipped with a reflux condenser and containing 4-(dimethylamino)pyridine (1.62 g, 13.3 mmol, 2.0 equiv) and freshly distilled dry pyridine (400 mL). The flask was heated by a surrounding bath to an internal temperature of 113 °C, the THF solution was added slowly with vigorous stirring over 18–24 h under N_2, and stirring was continued at 113 °C for 6 h. The solution was then cooled and evaporated to yield a brown oil that was dissolved in $CHCl_3$. The solution was washed (1 M HCl, 3 × 25 mL; aqueous $NaHCO_3$, 3 × 25 mL; brine, 25 mL; all aqueous phases were back extracted with $CHCl_3$, and the organic phases were pooled). Evaporation yielded crude product, 920 mg. Analysis by TLC (7:3 EtOAc–MeOH) revealed two major UV inactive bands, R_f 0.41 and 0.62, along with a minor UV inactive band, R_f 0.52. Isolation of the major bands by flash chromatography (9:1 EtOAc–MeOH) yielded 276 mg (28%) of the 2*S*,5*S*,8*S*,11*S* isomer **2a** as an oil, R_f 0.62, and 309 mg (31%) of the 2*S*,5*R*,8*R*,11*S* isomer **16** as a solid: mp 123–128 °C dec, R_f 0.41, $[\alpha]_{589}$ −13.4° (*c* 1.35, MeOH).

For repeated or large-scale preparations, the diastereomers are more conveniently separated by preparative reversed-phase HPLC on a Vydac C_{18} column. The residues obtained from evaporation of the $CHCl_3$ solution after extractive workup were swirled in aqueous MeCN (7:3, 5 mL), and the resulting solution was freed of fine insolubles by passage through a C_{18} separatory cartridge (Waters), which is then rinsed with several portions of solvent. The combined effluents were condensed to ca. 8 mL and sequentially loaded in 1.0 mL portions onto the column: mobile phase 13% MeCN–87% H_2O (0.1% TFA); flow rate, 18 mL/min, 214 nm detection; t_R of 2*S*,5*S*,8*S*,11*S* isomer, 12.2 min. t_R of 2*S*,5*R*,8*R*,11*S* isomer, 8.5 min. Near-base-line separation was achieved. In an alternative separation procedure, the diastereomeric ester mixture was saponified as described below, and the resulting acids were separated by preparative reversed-phase HPLC: ^1H NMR of the 2*S*,5*R*,8*R*,11*S* isomer **16** ($CDCl_3$, 300 MHz) δ 4.69 (1 H, dd, *J* = 2.5, 8.8 Hz), 4.68–4.60 (1 H, m), 4.62 (1 H, d, *J* = 7.5 Hz), 3.85–3.75 (2 H, m), 3.79 (3 H, s), 3.50 (1 H, d, *J* = 11.7 Hz), 3.09 (1 H, dd, *J* = 5.6, 16.0 Hz), 2.86 (1 H, d, *J* = 15.4 Hz), 2.51–2.36 (2 H, m), 2.36 (3 H, s), 2.14–2.04 (2 H, m), 1.99–1.92 (2 H, m), 1.91–1.86 (1 H, m); HRMS calcd for $C_{14}H_{20}N_2O_4S$ 312.1143, found 312,1145.

B. Preparation and Characterization of the 2*S*,5*S*,8*S*,11*S* Isomer 2a. The above reaction sequence was repeated using *trans*-1-(*tert*-butoxycarbonyl)-2(*S*)-(methoxycarbonyl)-5(*S*)-[(tosyloxy)methyl]pyrrolidine (*S,S*)-**5** to generate solely the R_f 0.62 isomer **2a** as an oil: $[\alpha]_{589}$ +11° (*c* 0.50,DCM); ^1H NMR ($CDCl_3$, 300 MHz) δ 4.67 (1 H, d, *J* = 8.7 Hz), 4.65 (1 H, d, *J* = 8.5 Hz), 4.38 (1 H, m), 3.83 (2 H, m), 3.74 (3 H, s), 3.61 (1 H, dd, *J* = 5.4, 5.6 Hz), 3.18 (1 H, dd, *J* = 5.1, 15.0 Hz), 2.78 (1 H, m), 2.58 (1 H, d, *J* = 13.7 Hz), 2.35–2.24 (1 H, m), 2.32 (1 H, dd, *J* = 10.0, 15.0 Hz), 2.20 (3 H, s), 2.11 (1 H, m), 1.96 (1 H, dd, *J* = 6.0, 12.8 Hz), 1.76 (1 H, dd, *J* = 6.0, 12.8 Hz). HRMS calcd for $C_{14}H_{20}N_2O_4S$ 312.1143, found 312.11446.

(2*S*,5*S*,8*S*,11*S*)-1-Acetyl-1,4-diaza-3-keto-5-carboxy-10-thiatricyclo[2.8.1.0^{4,8}]tridecane 2b. A solution of the above prepared methyl ester **2a** (61.0 mg, 0.19 mmol, 1.0 equiv) in aqueous NaOH (0.10 M, 3.0 mL) was stirred for 6 h at 23 °C, checked by HPLC for complete reaction of starting material, acidified to pH 1 with HCl, and evaporated. The solid residue was dissolved in H_2O (2 mL) and purified by reversed-phase preparative HPLC. (mobile phase, 8% MeCN–92% H_2O (0.1% TFA); flow rate, 18 mL/min, 214 nm detection; t_R 10.5 min; t_R of 2*4S*,5*R*,8*R*,11*S* isomer 6.8 min). The oil **2b** obtained by evaporation of the eluant (44 mg, 75%) crystallized on standing and could be recrystallized from a minimum volume of water (large prisms) or from a minimum volume of EtOH (tiny needles), mp 238–244 °C. The compound **2b** is readily soluble in H_2O, DMF, DMSO, and MeOH, but sparingly soluble or insoluble in ether, DCM, $CHCl_3$, EtOAc, Me_2CO, dioxane, or toluene: FAB MS *m/e* 299 (MH^+); ^1H NMR (D_2O, 500 MHz, 2 conformations present) δ 4.71 (0.6 H, d, *J* = 6.0 Hz), 4.56 (0.6 H, d, *J* = 7.0 Hz), 4.45 (0.4 H, d, *J* = 7.0 Hz), 4.31 (1 H, m), 4.00 (1 H, m), 3.81 (1 H, m), 3.75 (1 H, m), 3.31 (1 H, 2dd, *J* = 6.0, 15.0 Hz), 2.85 (0.6 H, m), 2.75 (0.4 H, m), 2.50 (1.6 H, m), 2.38 (0.4 H, d, *J* = 14.0 Hz), 2.25 (2 H, m), 2.14 (3 H, 2 s), 2.05 (1 H, m), 1.88 (1 H, m). (For X-ray structural data, see Discussion and supplementary material.)

NMR Studies of 2b in D_2O. The samples of NOE studies were lyophilized repeatedly from D_2O. For the last two lyophilizations, solvent of 99.996% isotopic purity was used (MSD isotopes). The final sample concentration was ca. 0.04 M.

All spectra were obtained at 500 MHz on a Varian VXR500S spectrometer, with data processing on a SUN3/60 workstation using Varian software. Difference NOE experiments[32] were run at 35.0 °C. Generally, 256 on- and off-resonance irradiated transients were collected in an interleaved fashion, employing a 3.5-s presaturation and a 1.0-s recycle delay. Line broadening (0.5 Hz) was applied to minimize Bloch-Siegert shifts.

All 2-D spectra were run in the phase-sensitive mode, employing the method of States et al.[33] The double-quantum-filtered COSY experiments[34] were run in D_2O at 25.0 °C. Each hypercomplex data set comprised 256 increments of 16 scans each, containing 2048 points per scan and run with a recycle time of 2.5 s. This protocol provided a digital resolution in ω_2 of approximately 1.0

(32) Hall, L.; Sanders, J. *J. Am. Chem. Soc.* **1980**, *102*, 5703–5711.
(33) States, D. J.; Habekorn, R. A.; Ruben, D. J. *J. Magn. Res.* **1982**, *48*, 286–292.
(34) Rance, M.; Sorensen, O.; Bodenhausen, G.; Wagner, G.; Ernst, R.; Wuethrich, K. *Biochem. Biophys. Res. Commun.* **1983**, *117*, 479–485. Neuhaus, D.; Wagner, G.; Vasak, M.; Kagi, J.; Wuethrich, K. *Eur. J. Biochem.* **1985**, *151*, 257–273.

Hz/data point over the 2155 Hz spectra width. The free induction decays were zero-filled to a final 2K×1K data matrix and transformed with Gaussian weighting in ω_2 and sifted-Gaussian weighting in ω_1.

ROESY experiments[35] were performed in D_2O at 25.0 or 35.0 °C using a pulsed spin lock[36] yielding an effective B_1 field strength of 790–930 Hz during the 300-ms mixing period. The 30° mixing pulse was preceded and followed by a hard 90° pulse for resonance offset compensation. To identify spurious Hartmann–Hahn transfer peaks the ROESY spectra were acquired with carrier frequency offsets varied by 280 Hz. Spectral widths were 2100–2500 Hz in both dimensions. For each hypercomplex data set, 16 scans of 256–300 increments were collected, with each increment described by 2048 data points. The FIDs were zero-filled to a 2K×1K data matrix and transformed with Gaussian or shifted-Gaussian weighting in ω_2 and with shifted Gaussian weighting in ω_1.

Molecular Modeling. Energy minimization calculations were carried out on a Silicon Graphics Personal Iris minicomputer using the Quanta 2.1 version of CHARMm marketed by the Polygen Corp. In order to avoid uncertainties in torsional strain estimates, all torsional angles in the .RTF file were redefined to exclude hydrogen atoms at the terminal positions. Energies of defined conformations were minimized by a sequence involving steepest descents, followed by conjugate gradient, ending with the adopted basis Newton-Rafeson algorithm. A conformational search using burst dynamics followed by minimization was applied to 40 structures to construct a complete list of conformations corresponding to local energy minima. To determine the effect of variations in bond energy parameters on relative energies, the bond stretching force constant for the C–C–S angles (three of which appear in the structure of **2**) was reduced by a factor of 0.8; no significant differences in conformational energies were observed. To determine the effect of charge parameters, calculations were carried out using either the Quanta default charge values for organic structures or the recommended charge for peptides (shown in parentheses) of +0.14 (+0.14), –0.29 (–0.35), +0.30 (+0.55), and –0.33 (–0.55) for the secondary amide H, N, C, and O, respectively. Total molecular charges were summed to zero by distributing surplus amide charge evenly over neighboring backbone atoms. The peptide values gave more realistic predictions of the energy differences discussed in the text. A radius-dependent dielectric model gave poorer agreement than a constant dielectric model. Either very low (ca. 1.0) or relatively high (>10) dielectric constants gave the best fit to the experimental results.

(35) Bothner-By, A.; Stephens, R. L.; Lee, J. *J. Am. Chem. Soc.* **1984**, *106*, 811–813. Bax, A.; Davis, D. *J. Magn. Res.* **1985**, *63*, 207–213.

(36) Kessler, H.; Griesinger, C.; Kerssebaum, R.; Wagner, K.; Ernst, R. *J. Am. Chem. Soc.* **1987**, *109*, 607–609.

Acknowledgment. We wish to thank Dr. Paul Bash for assistance with the molecular modeling programs and Drs. Frank Momany and Joe Klimkowski of Polygen Corp. for supplying parameters and for helpful advice concerning the implementation of QUANTA/CHARMm. Financial assistance from the National Science Foundation (Grant 8813429-CHE) and from Pfizer Inc. is gratefully acknowledged.

Registry No. 2a, 119888-29-8; **2b**, 120980-87-2; **2c**, 136175-21-8; (*S,S*)-**5**, 120980-88-3; (±)-**5**, 136235-07-9; (±)-**5** (5-hydroxymethyl derivative), 136175-14-9; **6**, 51-35-4; **6**·HCl (methyl ester), 40216-83-9; *N*-acetyl-**6** (methyl ester), 67943-19-5; **7**, 57750-51-3; **7** (free acid), 100895-61-2; **8**, 78854-23-6; (±)-**9**, 90290-04-3; (±)-**10**, 136201-47-3; (±)-**10** (diethyl ester), 136175-13-8; (*S*)-**11**, 86661-32-7; (±)-**11**, 136235-11-5; (2*S*,4*S*,21*S*)-**12**, 136175-11-6; (2*S*,4*S*,21*S*)-**12** (*p*-nitrophenyl ester), 136175-18-3; (2*S*,4*S*,21*R*)-**12**, 136175-20-7; (2*S*,4*S*,21*R*)-**12** (*p*-nitrophenyl ester), 136175-19-4; **13**, 136175-12-7; **14**, 136235-08-0; (2*S*,5*S*,8*S*,11*S*)-**15**, 120980-90-7; (2*S*,5*S*,8*S*,11*S*)-**15** (*p*-nitrophenyl ester), 136175-17-2; (2*S*,5*R*,8*R*,11*S*)-**15**, 136314-75-5; (2*S*,5*R*,8*R*,11*S*)-**15** (*p*-nitrophenyl ester), 136235-09-1; **1b**, 136235-06-8; **1b** (free acid), 136235-10-4; $PhCH_2SH$, 100-53-8; (+)-ephedrine, 321-98-2; (±)-*trans*-1-benzylpyrrolidine-2,5-dicarboxylic acid, 93713-33-8; (2*S*,2*S*)-1-benzylpyrrolidine-2,5-dicarboxylic acid, 136175-15-0; (2*S*,5*S*)-1-benzylpyrrolidine-2,5-dicarboxylic acid dimethyl ester, 118396-01-3; (2*S*,5*S*)-1-(*tert*-butoxycarbonyl)pyrrolidine-2,5-dicarboxylic acid dimethyl ester, 126640-85-5; (2*S*,5*S*)-1-(*tert*-butoxycarbonyl)-5-(methoxycarbonyl)pyrrolidine-2-carboxylic acid, 120980-89-4; (2*S*,5*S*)-1-(*tert*-butoxycarbonyl)-5-(hydroxymethyl)pyrrolidine-2-carboxylic acid, 136175-16-1.

Supplementary Material Available: Details of X-ray crystallographic analysis of Ac–Hel_1–OH; details of instrumentation used for experimental studies; experimental synthesis and characterization of compounds **13**, **14**, and **15** (7 pages). Ordering information is given on any current masthead page.